available at www.sciencedirect.com

ScienceDirect

journal homepage: www.elsevier.com/locate/agwat

# Rain Infiltration into swelling/shrinking/cracking soils

*M.J.M. Römkens* [a,*], *S.N. Prasad* [b]

[a] *USDA-ARS National Sedimentation Laboratory, P.O. Box 1157, 598 McElroy Drive, Oxford, MS 38655, United States*
[b] *The University of Mississippi, Department of Civil Engineering, University, MS 38677, United States*

ARTICLE INFO

*Article history:*
Accepted 19 July 2006
Published on line 18 September 2006

*Keywords:*
Rain infiltration
Swelling/shrinking/cracking soils

ABSTRACT

A model for predicting rain infiltration at the field scale with swelling/shrinking/cracking/ soils is described. The simplifying assumptions are: (1) no vertical infiltration takes place due to a sealed surface condition. rainwater moves laterally over the soil surface to the cracks, where it uniformly flows along the vertical walls of the cracks. (2) The geometry is represented by a prismatic column structure with cracks between the columns. The approach consists of a two-component process of Darcian matrix flow in the soil medium and Hortonian flow on the walls of the cracks. The Darcian analysis of horizontal matrix flow uses a spectral series solution of the Richards equation for the wetting front advance. The crack volume is determined from bulk density measurements, from which ponding time estimates can be made. Closed-form expressions are derived for the cumulative infiltration. The analytical results are compared with experimental results obtained for a Mississippi Delta clay soil. For the case, where excess rainwater has reached the bottom of the crack at the moment crack closure occurs, an exact solution is obtained for incipient ponding as a function of crack morphology, rainfall intensity, and sorptivity. Runoff is computed as the difference between the cumulative rainfall and cumulative infiltration.



## 1. Introduction

There is a great need to improve infiltration predictions into swelling/shrinking/cracking soils at the field and watershed scale. Since the early analytical work by Smiles and Rosenthal (1968), Philip (1974), and Smiles (1974), significant progress on fundamental aspects concerning infiltration into swelling soils has been made, yet much more needs to be done. One of the most challenging tasks is to predict infiltration into swelling/shrinking/cracking soils at the field scale that contain significant amounts of swelling clays and are commonly found in soils on highly productive agricultural land. These soils often exhibit large cracks that can be several cm wide and as much as 1 m deep. These cracks may absorb large amounts of rainwater during the early stages of a rainstorm event, that occurs as preferential flow and delay runoff initiation. While preferential flow may occur on any soil, even sandy soils, the most common occurrence is on non-disturbed fine textured soils through the existing macro-pores (cf. Bouma, 1991; Beven and Germann, 1982; Askar and Jin, 2000) or through shrinkage cracks (Bronswijk, 1988; Kutilek, 1996; Kim et al., 1999; Greco, 2002). Generally three morphologically based infiltration pathways are recognized: matrix flow, macro-pore flow, and flow into shrinkage cracks. Their relative significance varies from case-to-case and depends on soil type and degree of soil disturbance or manipulation.

Matrix flow for a rigid soil medium has been amply studied by soil physicists and hydrologists, following the formulation of the Richards equation in 1931 (for brief reviews see Philip, 1974, and Raats, 2001). Quantifying flow in non-rigid soils

* *Corresponding author*. Tel.: +1 662 232 2940; fax: +1 662 232 2915.
E-mail address: mromkens@ars.usda.gov (M.J.M. Römkens).
0378-3774/$ – see front matter 
doi:10.1016/j.agwat.2006.07.012

offers much greater challenges (Raats, 2002), especially in the presence of macro-pores and cracks. Macro-pore flow often plays a dominant role in drainage of agricultural fields. This flow is not adequately described.

The practical importance of swelling/shrinking/cracking soils on field hydrology and topography was illustrated in a recent study by Kirby et al. (2003), in which large amounts of water storage and topography changes were observed. Several rather similar process oriented studies of infiltration into swelling/shrinking/cracking soils have been made. Hoogmoed and Bouma (1980) conducted a laboratory rainfall simulation study with 20 cm × 20 cm diameter undisturbed soil columns of a Dutch riverine soil. They identified three modes of water movement: (i) vertical matrix infiltration into the soil surface, (ii) gravitational flow of excess rainwater at selected places along bands on the vertical walls of the cracks, and (iii) absorption into the prismatic columns of the free water on the crack surface by matrix flow. The prismatic columns are defined as the soil volume surrounded by the cracks. Their results indicated that absorption into columns was extremely small, in part because of the relatively few flow ''bands'' of water that covered the vertical crack surfaces. The largest contribution of water intake into the soil columns was from vertical infiltration through the soil surface. However, most of the rainwater drained as by-pass flow through the continuous cracks of the sample and exited through the bottom of the sample. An important aspect of their study was the introduction of the rainfall intensity dependent contact area or ''band'' surface on the vertical walls which earlier was introduced and tested with dye by Bouma et al. (1978). Bronswijk (1988) discounted absorption into columns altogether and partitioned rainfall into vertical infiltration through the soil surface and direct rainfall entering the crack plus the rainfall that exceeds the infiltration capacity of the soil surface, running into the cracks. Excess rainfall is simply allowed to accrue to groundwater. An important aspect of this study is the recognition of subsidence and swelling aspects. Greco (2002) approached infiltration into swelling/shrinking/cracking soil from the perspective of two interacting flow domains: matrix flow dominated by Darcy-like flow and flow in macro-pores and shrinkage cracks with flow of the kinematic wave type. Greco's model has a lot of elements in common with the infiltration concepts of Hoogmoed and Bouma (1980), Bronswijk (1988), and Kutilek (1996), but provides more analytical details of the flow along the crack walls. Greco's model was tested on large, undisturbed soil columns in which excess rainwater was allowed to drain through the bottom surface. Water in dead-end pores, which extended to various depths, was simply allowed to be absorbed into the surrounding soil matrix.

In this article we discuss our research of rain infiltration into a swelling/shrinking/cracking Mississippi soil with high clay content that simulates seedbeds during a series of rainstorm events. The approach has a lot in common with the model for flow of water in vertisols described by Kutilek (1996), though the analysis differs. The experimental findings are complemented with an analysis of water flowing into cracks in the absence of free drainage. This research was conducted against the background of a need to partition rain into runoff and groundwater accrual in watershed.

## 2. Experimental methods

Preliminary experiments were conducted on a Mississippi swelling/shrinking/cracking soil that was subjected to a series of simulated rainstorms of 30 mm/h intensity and 3 h duration. In some experiments a different rainfall intensity was used (Table 1). An air dry Sharkey clay soil (very fine, smectitic, thermic, Vertic Haplaquepts), crushed and sieved to pass a screen with 2 mm openings, was packed in incremental stages to a density of about 1.40 g/cm$^3$ in a plexi-glass box of 65.0 cm × 85.0 cm × 15.0 cm. At the bottom of the box was a 2.5 cm fine sand layer in which perforated PVC pipes were embedded to allow for free drainage. The soil consisted of 65% clay, 32% silt, and 3% sand. The box was placed on a weighing platform (H90-5150 Model, Fairbanks Scales, Kansas City, MO) with load cell that allowed continuous monitoring of weight changes during rainfall and the subsequent drying phase with a resolution of 0.05 kg. The maximum load was 450 kg. The box had 2% slope steepness and the surface was initially smooth. The upslope and side slope edges of the box were provided with strips of molding clay to prevent local surface water runoff during the rainstorm event. All runoff was collected manually and in full at the lower side of the box, initially on a continuous basis and later on during the storm event on an intermittent basis. Following each rainstorm the box with soil was allowed to dry for an extended period of time, either passively by standing in ambient conditions or actively by blowing heated air over the soil surface. After soil bed preparation and at various drying stages after each rainstorm, surface topography changes due to wetting and drying were determined by measuring surface elevations on a 0.1 cm × 0.1 cm grid with a non-contact infrared laser (Römkens et al., 1988).

Complementary experiments were conducted for information about water absorption rates and wetting front penetration. A specific experiment was designed for wetting front depth determinations using an especially designed needle penetrometer (Wells, 2003). This technique is based on the fact that a syringe needle loaded with a 500 g weight penetrated through the wetted part of the sample. For soil used in this study, the depth of the wetting front could be equated with the penetration depth of the needle penetrometer. Penetrometer transects immediately after wetting and following drying were chosen at exactly this same location on the sample. This technique was very helpful in determining the rain infiltration depth in cracking clay soil. The water absorption rate of the Sharkey soil was determined on 26-cm diameter cylindrical columns, packed in the same manner as the sample box. Wetting of the sample occurred under zero tension at the bottom of the column by supplying water through a Mariotte arrangement. To determine the time course of the cumulative infiltration, the column was placed on a continuously weight recording balance. Wetting front advance was periodically measured by visual inspection.

## 3. Results of experiments

The cumulative infiltration for three successive rainstorms on sample 3 is shown in Fig. 1, while Table 1 summarizes the

**Table 1 – Simulated rainstorm characteristics, incipient ponding, drying time, and crack size for a prepared Sharkey-clay**

| Date (d-m-yy) | Sample** | Storm event | Rain intensity (mm $h^{-1}$) | Storm duration (h) | Drying time (d-h-m) | Incipient ponding (min) | Crack depth* (mm) | Crack width (mm) |
|---|---|---|---|---|---|---|---|---|
| 1-5-95 | 1 | 1 | 30 | 3 | 1-16-20 | 5 | N.D. | N.D. |
| 3-5-95 | 1 | 2 | 30 | 3 | 1-16-25 | 12 | N.D. | N.D. |
| 5-5-95 | 1 | 3 | 30 | 3 | 1-16-25 | 15 | N.D. | N.D. |
| 7-5-95 | 1 | 4 | 30 | 3 | 1-16-25 | 21 | N.D. | N.D. |
| 8-5-95 | 1 | 5 | 30 | 3 | 11-8-0 | 39 | N.D. | N.D. |
| 26-5-95 | 2 | 1 | 30 | 3 | – | 8 | N.D. | N.D. |
| 27-5-95 | 2 | 2 | 30 | 3 | 1-0-15 | 11 | N.D. | N.D. |
| 29-5-95 | 2 | 3 | 30 | 3 | 1-18-15 | 19 | N.D. | N.D. |
| 2-6-95 | 2 | 4 | 30 | 3 | 3-21-0 | 22 | N.D. | N.D. |
| 5-6-95 | 2 | 5 | 30 | 3 | 2-17-12 | 26 | N.D. | N.D. |
| 8-6-95 | 2 | 6 | 30 | 3 | 2-16-15 | 35 | N.D. | N.D. |
| 27-6-95 | 2 | 7 | 30 | 3 | 18-19-0 | 65 | N.D. | N.D. |
| 17-7-95 | 2 | 8 | 30 | 3 | 19-22-0 | 32 | N.D. | N.D. |
| 13-9-95 | 3 | 1 | 30 | 3 | – | 7 | N.D. | N.D. |
| 19-9-95 | 3 | 2 | 30 | 3 | 5-22-0 | 22 | N.D. | N.D. |
| 29-9-95 | 3 | 3 | 30 | 3 | 9-20-0 | 32 | N.D. | N.D. |
| 13-10-95 | 3 | 4 | 30 | 3 | 13-20-0 | 46 | N.D. | N.D. |
| 17-10-96 | 4 | 1 | 20 | 3 | – | 43 | N.D. | N.D. |
| 29-10-96 | 4 | 2 | 20 | 3 | 12-0-0 | 64 | N.D. | N.D. |
| 25-11-96 | 4 | 3 | 20 | 3 | 27-0-0 | 101 | N.D. | N.D. |
| 11-12-96 | 4 | 4 | 20 | 3 | 16-0-0 | 105 | N.D. | N.D. |
| 10-4-97 | 5 | 1 | 20 | 3 | – | 32 | N.D. | N.D. |
| 4-6-97 | 5 | 2 | 20 | 3 | 55-0-0 | 87 | N.D. | N.D. |
| 10-7-97 | 5 | 3 | 20 | 3.5 | 36-0-0 | 154 | N.D. | N.D. |
| 20-8-97 | 5 | 4 | 20 | 4.33 | 41-0-0 | 175 | N.D. | N.D. |
| 26-9-97 | 5 | 5 | 20 | 3 | 35-0-0 | 113 | N.D. | N.D. |
| 2-10-97 | 5 | 6 | 20 | 3 | 8-0-0 | 51 | N.D. | N.D. |
| 3-11-97 | 5 | 7 | 20 | 4 | 42-0-0 | 68 | N.D. | N.D. |
| 8-12-97 | 5 | 8 | 20 | 3 | 35-0-0 | 42 | N.D. | N.D. |
| 11-12-99 | 6 | 1 | 30 | 3 | – | 4 | | |
| 20-12-99 | 6 | 2 | 30 | 3 | 9-0-0 | 14 | 30 | 13 |
| 11-1-00 | 6 | 3 | 30 | 3 | 21-0-0 | 27 | 52 | 13 |
| 1-2-00 | 6 | 4 | 30 | 3 | 21-0-0 | 39 | 68 | 12 |
| 24-2-00 | 6 | 5 | 30 | 3 | 24-0-0 | 29 | 65 | 14 |
| 20-5-00 | 6 | 6 | 30 | 3 | 87-0-0 | 40 | 83 | 14 |
| 23-6-00 | 6 | 7 | 20 | 3 | 31-0-0 | 33 | 90 | 13 |
| 6-7-00 | 6 | 8 | 30 | 3 | 13-0-0 | 27 | 92 | 14 |

*ND: not determined; **box size for samples 1, 2, 3, and 4, was 65 cm × 85 cm × 15 cm, and for samples 5 and 6, it was 76.5 cm × 80 cm × 30 cm. Also, data from samples 1, 2, and 3 were from Wells (1995); data from samples 4 and 5 were from Neely (1998), and data from sample 6 were from Wells (2003).

experimental data for all runs and includes application rate, incipient ponding time, the drying period since the last storm event, and measured morphological aspects of the cracks. Fig. 2 shows a typical cracked Sharkey clay soil after several wetting and drying cycles. Each of the samples shows a very similar hydrologic response to a series of successive storm events. This response can be summarized as follows: (1) incipient ponding during the first storm on the initially packed dry soil material occurred at about 5–8 min into the storm. (2) Cracking occurred during the drying period following each rainstorm. Visual and penetrometer data (Wells, 2003) indicated that crack depths were very similar to the wetting front depths. (3) With each subsequent storm, the ponding time and cumulative infiltration increased, while the cracks became wider and deeper during the subsequent drying period. As a result, by the third storm on sample 3 the first 32 min of rainfall was fully absorbed by the sample (Fig. 1).

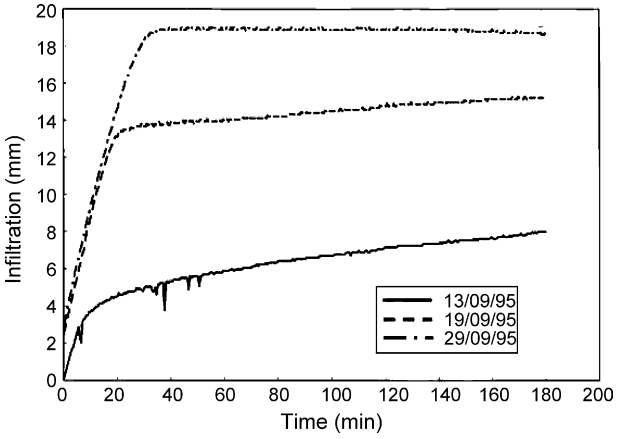


**Fig. 1 – Cumulative infiltration as a function of time for three successive rainstorms each of 3 h duration and 30 mm/h rainfall intensity (Wells, 1995).**

**Fig. 2 – Physical image of a cracking pattern after several wetting and drying cycles for a Sharkey clay soil. The largest column size is about 12 cm.**

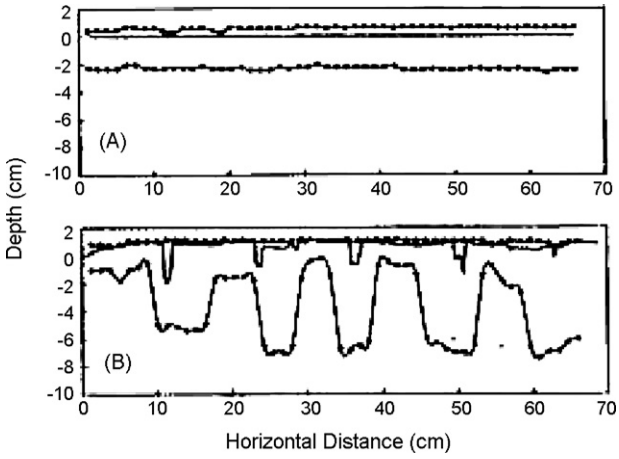


**Fig. 3 – Normalized surface elevation and penetration measurements following a series of simulated rainstorms on a Sharkey clay soil: (A) after the first rainstorm; (B) after the third rainstorm. The solid line represents the surface elevation prior to the rainstorm, the solid line with solid circle symbols represent the surface elevation immediately after the rainstorm prior to penetration, and the solid line with solid triangle symbols represents the final penetration depth (Wells, 2003).**

Similarly, the first 65 min of rainfall of the seventh storm on sample 2 was fully absorbed.

It appears that depending on cultivation history, rainstorm frequency, and drying period between storm events, incipient ponding is largely related to the crack morphology, e.g. spacing, width, and depth. Another feature shown in Fig. 1 is a change in the infiltration characteristics of the sample with subsequent storms. While during the first rainstorm on the freshly prepared sample the infiltration relationship is curvilinear, very much resembling those of non-swelling soils, the infiltration relationships of subsequent events show fairly abrupt changes in the infiltration rates. The most conspicuous change in Fig. 1 was noted for the infiltration relationship of the third storm event at a point in time that incipient ponding occurred. Until this point, the slope of the infiltration relationship is constant indicating that all rainfall is fully absorbed into the soil either by matrix infiltration or by flowing into the cracks or both. Following incipient ponding, cracks are either closed or filled directly by rainfall or by runoff water from the surface area between the cracks and the infiltration rate is drastically reduced. The nearly horizontal limit of the third storm event suggests that no rain at that point enters the soil and that thus all additional rain runs off from the sample. Visual observation indicated full closure of the cracks, while the sample surface had the appearance of a fully developed surface seal. In fact, the slope after about 30 min into the storm is decidedly negative, indicating a net soil loss by splash and runoff. The measured amount of soil in runoff was 0.017 g/cm$^2$/h, which agrees very well with the estimated weight reduction of the box of about 0.016 g/cm$^2$/h. Of all the runs, only storm 6 of sample 5 showed crack development that extended from the surface to the base of the sample. During that storm, drainage through the perforated pipes was noted and measured. At the end of the storm, about 25% of the applied rain had been removed through deep drainage.

Fig. 3 shows the results of the measured surface elevations and needle penetrometer measurements after the first and third rainstorm. The data indicate that the wetting front depth following the first rainstorm on an initially dry, uniformly prepared sample is smooth. Also, uniform vertical swelling is noted of approximately 5 mm and the wetting front depth was approximately 2 cm (Fig. 3A). Significant changes in wetting front depth were noted following the third rainstorm. The wetting front depth is highly irregular and follows the cracking pattern, while surface elevation changes, probably because of surface sealing effects, were almost imperceptible (Fig. 3B). Because of the triangulation type elevation measurements of the laser method, the bottom of the cracks could not be ascertained, though the crack location could be identified. Instead, a graduated scale was inserted in the cracks and their depth was determined. The graphs in Fig. 3B, which were obtained at exactly the same location as that of Fig. 3A, clearly indicate that the wetting depth was largest in regions of former cracks. These depths were approximately 7 mm, consistent with the graduated scale measurements. The trapezoidal shape of the penetrometer data relationship indicates that the wetting front closely followed the crack shape. If anything, the wetting front depth near the crack at the surface of the sample was deeper than at the bottom, suggesting that wetting of the soil in the crack area started at the surface and proceeded downward. Other penetrometer data of transects at different locations on the sample showed similar results. However, more data are needed with samples subjected to different rainfall intensity regimes to ascertain the possibility of cracks filling from the bottom up with high rainfall intensity storms.

All runs showed a limited amount of matrix infiltration through the soil surface. The largest amount occurred during the first storm on the freshly prepared sample and was estimated at about 30 mm, which is 1/3 of the applied rain. Subsequent rainstorms showed much less matrix infiltration through the soil surface.

Finally, the residual water content following drying increased gradually as determined by the intersect of the infiltration curves for the second and third rainstorm with the ordinate (Fig. 1).

## 4. Modeling infiltration into cracking soils

### 4.1. *Qualitative description of the model*

The data indicate that there are several modes of rainwater disposition: (1) rain is directly absorbed through the soil surface. (2) Rain falls directly into the cracks and is subsequently either absorbed into the soil columns or into the zone below the cracks. (3) Once surface ponding occurs, excess rainwater that accumulates on the column surface, runs uniformly into the cracks along the perimeter of the vertical column surfaces. The instant that water ponds on the column surface is called the matrix ponding time, $t_m$. (4) Runoff occurs, when cracks are filled or closed due to swelling of the soil matrix. This instant is designated as the field ponding time, $t'_p$. From the standpoint of runoff, $t'_p$ is an important and much desired parameter that needs to be determined in relation to the rainfall intensity, the morphological characteristics of the soil cracks such as spacing, depth, and width, and the soil absorption characteristics.

Crack sizes vary among soil types and depend on soil wetness. In soils with high clay content and a considerable amount of clay minerals of the swelling type, i.e., the group of smectite clays, cracks may be several cm wide and extend to great depth, and be closely spaced (Fig. 2). In soils with lower clay content and clay minerals with less swelling, i.e., kaolinite, vermiculite, etc., or in soils with matrix contraction due to negative soil water pressures, the cracks are much narrower and may even be of the hair line type. Depending on the rainfall intensity, the mode of infiltration may differ between these two cases. In the first case, rainwater moves probably at selected places directly into the cracks and the cracks fill up from the bottom with lateral absorption taking place into the wetted parts of the crack surface and the crack bottom. In the second case, water will most likely enter at the perimeter of the crack as film flow and will immediately be drawn laterally into the soil columns. Thus, wetting takes place ''layer-wise'' from the top of the column downward. This scenario is supported by the penetrometer data (Fig. 3B) which indicated more advanced lateral wetting in the top layer of the column as compared to the layers in the lower part of the column. Model assumptions are: (1) for the fine pulverized, compacted soil with particle sizes less than 2 mm and a high content of swelling clay, water entry into the soil matrix is assumed to be exclusively by diffusive flow: (2) infiltration through the soil surface was negligible because of sealing due to the structure destructive effect of impacting rain drops. (3) Water flow along the vertical surfaces of the soil columns is uniform over its circumference. (4) Horizontal infiltration is taking place from the vertical surfaces inward. (5) Wetting front advance interactions between adjacent vertical crack surfaces are assumed to be negligible. In this study, field ponding time $t'_p$ was a good measure of crack closure.

A sketch of the model is given in Fig. 4. The geometry of the polygonal columns is assumed to be quadrangular with sides of width $\ell$ and height $H$. The initial soil water content is assumed to be zero, so that the amount of water, $q_o$, entering

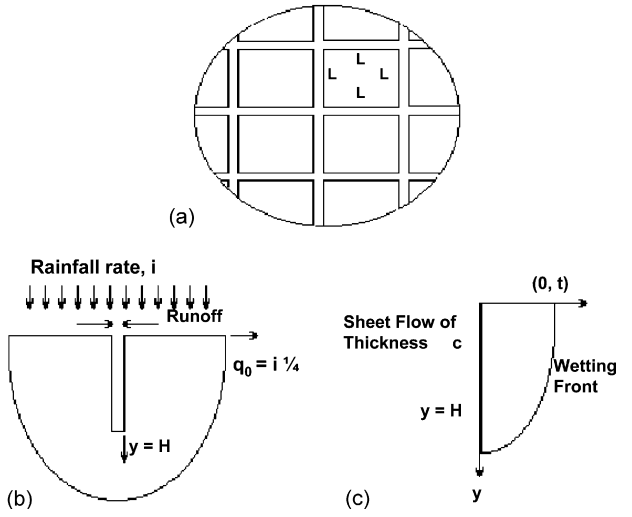


**Fig. 4 – A geometric representation of the infiltration model: (a) horizontal cross-section of the cracked profile; (b) vertical cross-section through crack area; (c) wetting front in a column adjacent to the crack.**

the soil column per unit column face width is given by the relationship:

$$q_o = \frac{i\ell^2}{4\ell} = \frac{i\ell}{4}, \tag{1}$$

where $i$ is the rainfall intensity. For a hexagonal column with equal sides, $q_o$ equals $1/4\ell i\sqrt{3}$. The model represents in effect a two-component, decoupled process of Darcian matrix flow in the soil medium and Hortonian flow on the walls of the cracks. The thickness of the film is dictated by either the kinematic wave equation or the St. Venant equation for flow on a sloping plane.

### 4.2. *Horizontal absorption into vertical surfaces of cracks*

Horizontal absorption into vertical surfaces of cracks is assumed to be described by the Richards equation in the form:

$$\frac{\partial\theta}{\partial t} = \frac{\partial}{\partial x}\left(D(\theta)\frac{\partial\theta}{\partial x}\right) \tag{2}$$

subject to the conditions:

$$\begin{aligned} &x = 0, \quad t > 0, \quad \theta = \theta_s, \quad D\frac{\partial\theta}{\partial x} = \text{finite}, \quad x > 0, \\ &t = 0, \quad \theta = 0, \end{aligned} \tag{3}$$

where $\theta$ is the reduced water content $\theta = (\theta - \theta_r)/(\theta_s - \theta_r)$, $\theta_r$ the residual water content, $\theta_s$ the water content at saturation, $D$ the diffusivity function, $t$ and $x$ are the time and space coordinates, respectively. The Richards equation, as formulated in (2), governs the water flow in a rigid medium in which ($x$, $t$) is the fixed coordinate system. For a non-rigid medium of the type used in this study, the flow equation needs to be modified to reflect the effect of the changing matrix. For those cases, a material coordinate is best used to describe the flow regime (Kim et al., 1999; Raats, 2002; Smiles, 1974; Smiles and Rosenthal, 1968). For

reasons of convenience and simplicity, we opted for an approximate, engineering approach by using the Richard equation as formulated.

Römkens and Prasad (1992) have shown that the solution of (2) subject to (3) can be expressed as a spectral series:

$$\theta(x,t) = A_0\left(1-\frac{x}{\delta_1}\right)^{\alpha} + A_1\left(1-\frac{x}{\delta_1}\right)^{\alpha+1} + A_2\left(1-\frac{x}{\delta_1}\right)^{\alpha+2} + \cdots, \quad (4)$$

where the coefficients $A_i$ for $i = 0, 1, \ldots$, are time dependent functions and $\delta_1$ is the wetting front depth (Römkens and Prasad, 1992) and $\alpha$ ($0 < \alpha < 1$) is a constant that describes the shape of the wetting front and the soil water content profiles. The solution technique includes the use of the Ahuja–Swartzendruber relationship (1972), which through its functional form and constants expresses the nature of the soil water transmission characteristic, while the spectral series expresses the nature of the soil water content profile especially near the wetting front tip through the constant $\alpha$. As has been shown by Römkens and Prasad (1992) $\alpha$ represents a direct linkage between the shape of the water content profile around the wetting tip and the diffusivity function (details of this analysis are given in Appendix A). The Ahuja–Swartzendruber relationship is given by:

$$D(\theta) = \frac{a\theta^n}{(\theta_s-\theta)^{n/5}} = \theta^n F(\theta), \quad (5)$$

implying

$$\theta = 0 \rightarrow D(\theta) = 0, \quad \theta = \theta_s \rightarrow D(\theta_s) = \infty, \quad (6)$$

where $a$ and $n$ are soil specific constants. From analytical consideration (Appendix A based on Römkens and Prasad, 1992), Eqs. (2), (4), and (5) yield important relationships: (i) $\alpha = 1/n$, and (ii) an expression (Eq. (A8)) for the wetting front advance. The wetting front advance is also given by:

$$\delta_1^2 = A^2 t \quad (7)$$

where $A^2$ is a soil parameter (Kirkham and Feng, 1949; Bruce and Klute, 1956) and has the dimensions [$LT^{-1/2}$]. Combining these relationships together with the concentration boundary condition (3) for this case yields the relationship:

$$A^2 = \frac{2a}{\theta_s^{n/5}}\alpha\left[\frac{1}{2}(\alpha+1)(\alpha+2)\theta_s\right]^n. \quad (8)$$

The cumulative infiltration into a horizontal slice of this column is given by:

$$I = \int_0^{\delta_1} \theta(x)\,dx, \quad (9)$$

which upon integration and the use of the above relationship yields:

$$I = \frac{3\theta_s}{3+\alpha}\delta_1 = \lambda\sqrt{t}, \quad (10)$$

where

$$\lambda = \frac{3\theta_s A}{3+\alpha}, \quad (11)$$

$\lambda$ is commonly referred to as the sorptivity. In this case, the analysis provides additional detail through (8) and (11) concerning the nature of the sorptivity relationship to the parameters $\alpha$, $a$, and $\theta_s$ of the Ahjua-Swartzendruber diffusivity function.

### 4.3. *Incipient ponding time*

By considering for a unit column face width the depth integrated mass balance, an expression may be obtained for the incipient ponding time. This depth integrated mass balance is obtained by equating the cumulative rainfall $q_o t$ to the sum of the amount of water in films of thickness $c$ on the column face and amount of water absorbed into the columns. The mass balance equation is:

$$q_o t = \int_0^h (I + c)\,dy. \quad (12)$$

Assuming the film thickness $c$ to be constant and regarding the amount of water at depth $h$ as a function of the time lapse $t - \tau$ where $\tau$ is the time the water film first appeared at depth $h$, gives (Prasad et al., 1999):

$$q_o t = ch + \int_0^t I(t-\tau)\frac{dy}{d\tau}d\tau. \quad (13)$$

Substitution of identity (10) and use of the Laplace transform yield from the solution of (13) the following expression (Prasad et al., 1999):

$$\frac{h}{q_o} = \frac{4\sqrt{t}}{\pi\lambda} + \frac{4c}{\pi\lambda^2}\left[\exp\left(\frac{\pi\lambda^2 t}{4c^2}\right)\operatorname{erfc}\left(\frac{\sqrt{\pi}\lambda\sqrt{c}}{2c}\right) - 1\right]. \quad (14)$$

Assume that at time $t$, the water film on the vertical surface of the column has reached the bottom of the crack and that the crack then has closed by swelling during the wetting process, ($c \rightarrow 0$), then $h \rightarrow H$ and $t \rightarrow t'_p$and relationship (14) reduces to:

$$\sqrt{t'_p} = \frac{\pi\lambda}{i}\frac{H}{\ell}, \quad (15)$$

where $t'_p$, is the field ponding time. This relationship shows that for this special case the field ponding time $t'_p$ is in an exact manner related to the morphological characteristics ($H$, $\ell$) of the crack pattern, the rainfall intensity $i$, and the sorptivity $\lambda$. The occurrence of this scenario depends on the relationship of the rainfall intensity and the swelling dynamics of the soil material. That is, the rainfall intensity must be such, that when the water film on the faces of the column reaches the depth $H$ (crack depth), crack closure occurs at the soil surface. For larger intensities and certainly for very large intensities one might argue that cracks may rapidly fill up with rainwater and runoff may occur before crack closure takes place: in other words that the soil swelling dynamics is slow in relation to the

water volume entering the cracks. On the other extreme, in cases of very low intensities, cracks may close at the surface, while deeper parts of the column are still dry, thus restricting free water entry. Eq. (15) provides a good estimate of the field ponding time for this special case. In order to arrive at an estimate of $t'_p$ for the more general case, a relationship involving $t_p$, $t'_p$, and $w$ (one-half of crack width) must be found. This relationship is in principle determined by the degree of coupling of matrix flow, in which a certain amount of rainwater is absorbed into the column from the water film on the crack surfaces, and the progression of the tip of the water film moving downward along the crack surface. Rainwater absorption by the soil matrix is primarily controlled by the soil hydraulic properties and the state of wetness, i.e., depth of the wetting fronts in the horizontal and vertical directions within the columns. Film flow is in essence controlled by the rainfall intensity with minor adjustments due to extraction of film water by the soil matrix. The development of this relationship poses mathematical challenges as it involves two-dimensional flow.

The overall dynamics of rainfall-runoff is represented by the inequality

$$q_o t \geq R_1^* + R_1, \tag{16}$$

where $R_1$ is the amount of water absorbed by the soil matrix through the crack faces and $R_1^*$ is that stored in the cracks. When the left side of (16) is smaller than the right hand side, no runoff takes place, whereas, when it is larger runoff continues. When $R_1^*$ fills up the crack volume, ponding occurs and runoff starts. Thus, some estimates may be made by equating the crack volume plus the volume of water infiltrating into the soil matrix for $t > t_p$ to the rainfall during this period $T$, algebraically defined as $T = t'_p - t_p$.

Fig. 5 shows a geometric approach for estimating the cumulative infiltration into the cracked soil. The following approximate relationship is obtained:

$$q_o(t'_p - t_p) = Hw + \frac{1}{4}\pi\delta^2(t'_p - t_p) + \int_0^H I(t'_p - t_p)\,dy. \tag{17}$$

The first term on the RHS of (17) represents the crack volume at the instant $t_p$. The second term is the bell-shaped infiltration volume below the crack. This volume is approximated by a quarter sector of a circle with radius $\delta(t'_p - t_p)$. Note that $\delta(t'_p - t_p)$ represents water depth. The assumption is made that for diffusive flow, the horizontal wetting front penetration equals that of the vertical wetting front penetration. The third term on the RHS of Eq. (17) represents the rainwater that laterally infiltrated into the soil matrix over the depth $H$ during the time interval $T$. Since $H = \delta(t_p)$ solving (17) for $w$ gives:

$$w = \frac{q_o T}{H} - \frac{1}{4}\pi A^2 \frac{T}{H} - I(t'_p - t_p). \tag{18}$$

It also can be shown by a series expansion and terms truncation that $\sqrt{T} = \sqrt{t'_p - t_p}$ can be approximated by

$$t_p = 2t'_p\left[1 - \sqrt{\frac{T}{t'_p}}\right]. \tag{19}$$

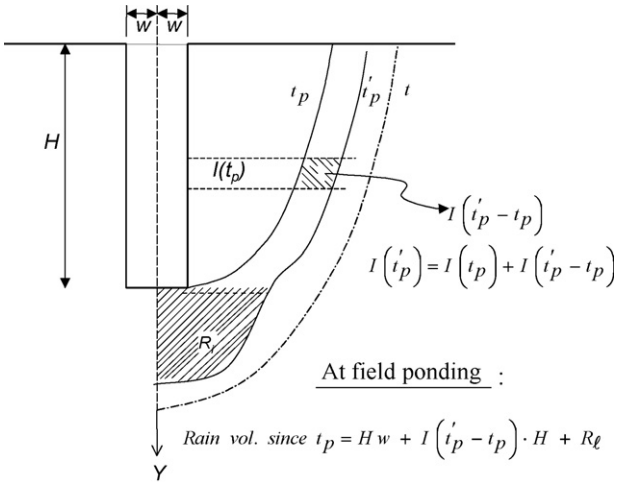


**Fig. 5 – A schematic representation of soil water content profiles in the crack area.**

Assuming that the soil column following a storm event is fully saturated, then the crack width can be estimated from changes in the soil bulk density using the relationship,

$$w = \frac{\ell}{2}\left(\sqrt{\frac{\rho_d}{\rho_w}} - 1\right), \tag{20}$$

where $\rho_d$ is the dry soil density and $\rho_w$ is the wet bulk density. If upon crack closure, the wetting front has penetrated only over a limited distance into the column (see Fig. 3B), a more accurate approximation for the crack width would be

$$w = \frac{\ell}{2}\left[\left(\frac{2\delta_1}{\ell} - 1\right)^2 + \frac{\rho_d}{\rho_w}\left[1 - \left(1 - \frac{2\delta_1}{\ell}\right)^2\right]\right]^{1/2} - \frac{\ell}{2}, \tag{21}$$

where $\delta_1 = \lambda\sqrt{t'_p}$. For the case that upon closure the column is completely wetted, $\delta_1 = (\ell/2)$ and (21) reduces to (20). Eqs. (18)–(20) or (21) allow estimates of $T$ in terms of $t'_p$ for known $\rho_d$ and $\rho_w$.

### 4.4. *Cumulative infiltration*

The cumulative infiltration into cracked soils, especially soils with large crack volumes, may involve storage of significant amounts of water in the cracks. Cracks on soils with expansive clays, such as Sharkey clay, may be 2–6 cm wide and 50–100 cm deep. These cracks must fill up or close before runoff occurs. The total amount of water absorbed during a storm thus includes matrix soil water in the columns and possibly "free" water in the soil cracks. If the cracks start filling with water before closure, deeper parts of the soil profile beyond the depth of the crack may absorb an appreciable amount of water in which the crack bottom acts as a line source. The total amount of water absorbed by the soil along and below the cracks can be expressed as:

$$R = \int_0^{t_p} I(t - \tau)\frac{dH}{d\tau}\,d\tau + \int_0^H I(t - t_p)\,dy + R_\ell, \tag{22}$$

On the right hand side of (22), the first term represents the water absorbed in the column at the moment $t_p$ the water film on the vertical surface reaches the bottom of the crack. This volume equals the cumulative rainfall up to the instant $t_p$ of ponding. The second term represents the water absorbed in the soil matrix over the crack depth $H$ for $t \geq t_p$. The third term, $R_\ell$ represents the amount of water absorbed in the region $y > H$ below the cracks. Following the procedure given by Prasad et al. (2001), the time $T$ is the time required to fill the crack volume or for the cracks to close.

Since the cumulative infiltration at field ponding time consists of the soil matrix water plus the water in the crack, Eq. (22) by using (7), (10), and $H = \delta(t_p)$ can now be written as:

$$R = q_o t_p + \lambda H\sqrt{t'_p - t_p} + \frac{\pi}{4}\frac{AT}{\sqrt{t_p}}, \quad \text{for} \quad t = t'_p, \tag{23}$$

where the first term on the RHS of (23) represents the water volume in the matrix at the instant the water film on the column surface reaches the bottom of the crack, the second term is the additional matrix water that infiltrated since that instant up to field ponding time, and the third term is the sub-crack matrix water. If expressed as the cumulative infiltration rate per unit soil surface area, $I_g$, this relationship becomes

$$I_g = it_p + \frac{4H\lambda}{\ell}\gamma\sqrt{T} + \gamma\frac{\pi}{\ell}\frac{AT}{\sqrt{t_p}}, \quad \text{for} \quad t = t'_p, \tag{24}$$

where $\gamma$, an adjustment factor, accounts for the changes in the evolving internal matrix structure due to the wetting and drying cycles and for other inequities due to approximations and simplifications. The parameter $\gamma$ appears to be changing monotonically with the number of wetting and drying cycles and varied numerically in our experimental studies from 0.10 to 0.30 (Wells, 2003). The cumulative infiltration for $t > t'_p$ may be given by:

$$R = q_o t_p + \gamma\lambda H\sqrt{t - t_p}\beta + \frac{\pi}{4}\gamma\frac{A(t - t_p)}{\sqrt{t_p}}\beta, \quad \text{for} \quad t \geq t'_p, \tag{25}$$

or

$$I_g = it_p + \frac{4H\lambda}{\ell}\gamma\sqrt{t - t_p}\beta + \gamma\frac{\pi}{\ell}\frac{A}{\sqrt{t_p}}(t - t_p)\beta, \quad \text{for} \quad t \geq t'_p. \tag{26}$$

Several infiltration scenarios may develop. If cracks are fully closed and a seal develops, infiltration ceases as is shown in Fig. 1 during the third storm event. In that case, Eq. (24) is the expression to be used. If water continues to infiltrate unrestricted in the crack area, Eqs. (25) and (26) are the operative relationships and $\beta = 1$. The parameter $\beta$ ($\beta \leq 1$) accounts for the degree of flow impairment that occurs due to flow restrictions that have come about in the crack area. The gap between the crack faces may vanish but cleavages may remain, permitting a Hele–Shaw flow type along them as opposed to the film flow in the initial stage. Values of $\beta < 1$ need to be estimated to account for the degree of crack closure and vary from case-to-case. The analyses of cumulative infiltration with $\beta = 1$ is appropriate for stable crack configurations without significant crack closure due to swelling.

Rainfall-runoff analysis of agricultural fields with swelling and cracking soils, thus, may be carried out by adopting the cumulative infiltration relationships per unit area as given by Eqs. (24) and (26). These equations contain parameters $H/\ell$, $\gamma$, $\lambda$ and ponding times $t_p$ and $t'_p$. The sorptivity term $\lambda$ reflects physical and hydraulic soil characteristics. Ponding times depend on $\lambda$, $H/\ell$, crack width $w$, and rainfall intensity $i$. $H/\ell$ and $w$ are morphological quantities which depend on the swelling and cracking soil characteristics.

Runoff rates on a per unit surface area basis can now be determined from the relationship.

$$r = i - I_g/t, \quad \text{for} \quad t > t'_p, \tag{27}$$

where $r$ is the runoff rate per unit area.

Fig. 6 shows the cumulative infiltration on a Mississippi Delta, Sharkey soil as a function of time during three sequential rainstorms of 20 mm/h intensity and 3–4.3 h duration. Each storm was separated by a drying period (Table 1). Only one of every 120 data points have been plotted. The $\gamma$ values by Prasad et al. (2001) were obtained by matching the predicted infiltration values with the experimentally determined values. The sub-crack infiltration component was not considered in their approach. Our calculations using the second and third terms of (18) with $A^2 = 0.50$, indicates that sub-crack water absorption during period $T$ is about 10% of the laterally absorbed infiltration. Improving estimates of $\gamma$-values based on the crack morphology at the instant $t_p$ requires greater detail of the crack dynamics in relation to rainfall intensity and soil dynamics relative to changes in crack width and depth during the time interval $0 < t < t_p$. This aspect was not pursued in this article but is the subject of future work. The calculation relationships of Fig. 6 show good agreement with the data points following adjustments with a factor $\gamma$.

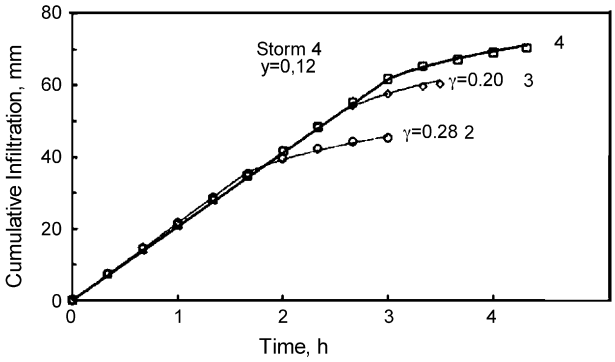


**Fig. 6 – Cumulative infiltration as a function of time for three successive rainstorms on a Sharkey clay; the lines represent the model calculations and the symbols represent observed data points. The observed data points in the linear portion of the graph represent every 120th observation, while those in the curvilinear portion of the graph represent every 60th observation (from Prasad et al., 2001).**

## 5. Concluding remarks

This study suggests that infiltration into highly complex swelling/shrinking/cracking soils can be estimated for field scale applications with process based predictive relationships of two interacting flow domains: matrix flow into the soil and macro-flow into cracks. The principal assumption made in the analysis was uniform flow of excess rain along the vertical walls of the crack surface with lateral imbibition into the soil. Experimental evidence of this study suggested that the first mode of infiltration governed by the infiltration process is dominated by lateral imbibition from the surface of the soil downward. It is possible that in other cases, particularly those with high rainstorm intensity, the lateral imbibition may occur from the bottom up. In that case, the zero pressure or concentration boundaries need to be modified in favor of a (time dependent) pressure head. More experiments and analysis need to be done over a wide range of rainfall intensities to better ascertain the prevalent infiltration mode. It is common knowledge that low rainfall intensities yield deeper wetted profiles than high intensity rain involving the same amount of rain. Thus, depending on rainfall intensity, crack depth and perhaps crack density will be affected differently during a subsequent rainfall event following a significant drying period.

Also, more attention must be paid to infiltration into the soil area immediately below the cracks and to deep drainage or other preferential flow paths. However, our experiments did not exhibit the latter features. One approach might be to view the crack tips as line sources. A major issue of concern in infiltration is the soil surface condition during rainstorms. This study was initiated with rain on an initially dry, pulverized but compacted soil material. Subsequent storms fell on the resulting undisturbed surface. Another major area of concern are changes in the micro-structure of the initially ground, though compacted soil during cycles of wetting and drying. This process may have a very substantial impact on the hydraulic characteristics of the soil especially at the wetting front. As a result infiltration by diffusive flow into the matrix, may be appreciable affected. Finally, a more definitive evaluation of infiltration into the soil using material coordinates could be pursued, though it must be recognized that the variation in the matrix constraining effect at different depth by the overburden would significantly complicate this matter. Because of the constraining effects, the end result may not necessarily be very different from what the present approach did yield. Thus, in-depth knowledge of cracking morphology is essential for an effective agricultural water management program.

## Acknowledgement

The authors deeply acknowledge the very helpful suggestions offered by Dr. P.A.C. Raats during the preparation of the manuscript.

## Appendix A

Richards' equation governs water movement in the soil profile. It must be satisfied at all points of the soil water profile including singular points such as at the tip of the wetting front and at other boundaries. The spectral series (Eq. (4)) can be written as:

$$\theta = \eta^{\alpha}\sum_{N=0}^{\infty} a_N(t)\eta^N = \eta^{\alpha} f(t,\eta) = a_0(\delta - x)^a + a_1(\delta - x)^{\alpha+1} + a_2(\delta - x)^{\alpha+2} + \cdots, \tag{A1}$$

where $a_i = A_i\delta^{-a}$ and $\eta = (\delta - x)$.

Substitution of Eq. (A1) into the Richards' equation for horizontal flow yields:

$$\alpha\eta^{\alpha-1}\frac{d\delta}{dt}f + \eta^{\alpha}\frac{\partial f}{\partial \eta}\frac{d\delta}{dt} + \mu^{\alpha}\frac{\partial f}{\partial t} = D\left\{\alpha(\alpha-1)\eta^{\alpha-2}f + 2\alpha\eta^{\alpha-1}\frac{\partial f}{\partial \eta} + \eta^{\alpha}\frac{\partial^2 f}{\partial \eta^2}\right\} + \frac{dD}{d\theta}\left\{\alpha^2\eta^{2\alpha-2}f^2 + 2\alpha\eta^{2\alpha-1}f\frac{\partial f}{\partial \eta} + \eta^{2\alpha}\left(\frac{\partial f}{\partial t}\right)^2\right\}. \tag{A2}$$

The singularity in the Richards' equation near the wetting front $z = \delta$ become obvious by noticing $\eta^{\alpha-1} \to \infty$ when $\eta \to \infty$, keeping in mind that the parameter $\alpha$ satisfies, $0 < \alpha < 1$. In order to find the contribution of the singular terms in unsaturated flow problems, we rewrite Eq. (A2) in the following form

$$\alpha\eta^{\alpha-1}f\frac{d\delta}{dt} + O(\eta^{\beta_1}) = D\alpha(\alpha-1)\eta^{\alpha-2}f + \frac{dD}{d\theta}\alpha^2\eta^{2\alpha-2}f^2 + O(\eta^{\beta_2}), \tag{A3}$$

where $\beta_i > 0$ and terms of the Order $\eta_i^{\beta}$ vanish near the wetting front $z = \delta$. A class of soil water diffusivity functions may be described by the relationship:

$$D(\theta) = \theta^n F(\theta), \tag{A4}$$

where $F(\theta)$ is a continuous function of $\theta$ and $F(0) \neq 0$, and n is a constant ($n \geq 1$). A typical diffusivity relationship that belongs to this class of functions and that will be considered in this article is the Ahuja–Swartzendruber diffusivity function for a non-swelling, stable soil matrix:

$$D(\theta) = \theta^n \frac{a}{(\theta_s - \theta)^{n/5}}, \tag{A5}$$

This function meets the requirement that $D(0) = 0$ and $D(\theta_s) = \infty$. $\theta_s$ is the saturated soil water content and $a$ is a constant.

When Eq. (A4) is utilized in Eq. (A3), we obtain the following singular terms of the Richards' equation:

$$\alpha\eta^{\alpha-1}f\frac{d\delta}{dt} + O(\eta^{\beta_1}) = \alpha(\alpha-1)\mu^{\alpha n+\alpha-2}f^{n+1}F + n\alpha^2\mu^{\alpha n+\alpha-2}f^{n+1}F + O(\eta^{\beta_2}). \tag{A6}$$

Thus, we may now equate the powers of $\eta$ from both sides of Eq. (A6) and also their coefficients to yield in the limit of $\eta \to 0$:

$$\alpha = \frac{1}{n}, \tag{A7}$$

and

$$\frac{d\delta}{dt} = \alpha f^{n}(t, o)F(O). \quad \text{(A8)}$$

Eq. (A7) shows the interdependency between the shape of the water content profile and the diffusivity function through the factor $\alpha$. Eq. (A8), however, is of a more fundamental nature and is referred as the dynamic equation governing the growth of the wetting front $\delta$. Thus, the wetting front propagation is influenced only by behavior of the diffusivity function $D(\theta)$ near $\theta \rightarrow O$ and the function $f(t, \eta)$ evaluated at $\eta = O$, the position of the wetting front tip.

It may be mentioned here that the evaluation of a well-defined wetting front takes place especially when the antecedent water content is relatively low. If the initial water content is appreciable then the wetting front diffuses in such a way that $D(\partial\theta/\partial x)$ remains finite everywhere and, therefore, $\alpha = O$. The solutions in these cases may be obtained by solving the system of equations as discussed in the earlier paper by Prasad and Römkens (1982).

## REFERENCES


Ajhuja, L.R., Swartzenbruber, D., 1972. An improved form of soil-water diffusivity function. Soil Sco. Soc. Am. Proc. 36, 9–14.

Askar, A., Jin, Y.-C., 2000. Macroporous drainage of unsaturated swelling soil. Water Resour. Res. 36, 1189–1197.

Beven, K., Germann, P., 1982. Macropores and water flow in soils. Water Resour. Res. 18, 1311–1325.

Bouma, J., 1991. Influence of soil macroporosivity on environmental quality. Adv. Agron. 46, 1–39.

Bouma, J., Dekker, L.W., Wösten, J.H.J., 1978. A case study on infiltration into dry clay soil. II Physical measurements. Geoderma 20, 41–51.

Bronswijk, J.J.B., 1988. Modeling of water balance, cracking and subsidence of clay soils. J. Hydrol. 97, 199–212.

Bruce, R.R., Klute, A., 1956. The measurement of soil moisture diffusivity. Soil Sci. Soc. Am. Proc. 20, 458–462.

Greco, R., 2002. Preferential flow in macroporous swelling soil with internal catchment: model development and applications. J. Hydrol. 269, 150–168.

Hoogmoed, W.B., Bouma, J., 1980. A simulation model for predicting infiltration into cracked clay soil. Soil Sci. Soc. Am. J. 44, 458–461.

Kim, D.J., Jaramillo, R.A., Vauclin, M., Feyen, J., Choi, S.I., 1999. Modeling of soil deformation and water flow in a swelling soil. Geoderma 92, 217–238.

Kirby, J.M., Bernardi, A.L., Ringrose-Voase, A.J., Young, R., Rose, H., 2003. Field swelling, shrinking, and water content change in a heavy clay soil. Aust. J. Soil Res. 41, 963–978.

Kirkham, D., Feng, C.L., 1949. Some tests of the diffusion theory and laws of capillary flow in soils. Soil Sci. 67, 29–40.

Kutilek, M., 1996. Water relations and water management of vertisols. In: Ahmed, N., Mermut, M. (Eds.), Vertisols and Technologies for Their Management. Developments in Soil Science. Elsevier, Amsterdam, The Netherlands.

Neely, R.M., 1998. Effect of surface condition on cracks and infiltration in a Mississippi Delta clay soil. M.S. Thesis. Department of Civil Engineering, University of Mississippi, University, MS.

Philip, J.R., 1974. Fifty years progress in soil physics. Geoderma 12, 265–280.

Prasad, S.N., Römkens, M.J.M., 1982. An approximate integral solution of vertical infiltration under changing boundary conditions. Water Resour. Res. 18, 1022–1028.

Prasad, S.N., Römkens, J.J.M., Wells, R.R., Neely, R., 1999. Predicting incipient ponding and infiltration into cracking soil. In: Proceedings of Nineteenth Annual Am. Geophys. Union Hydrology Days, Colorado State University, pp. 343–356.

Prasad, S.N., Römkens, M.J.M., Wells, R.R., 2001. Modeling cumulative infiltration into cracking soils. In: Proceedings of mposium on Preferential Flow. ASAE, Hawaii, January 2001, pp. 121–124.

Raats, P.A.C., 2001. Development in soil-water physics since the mid 1960s. Geoderma 100, 355–387.

Raats, P.A.C., 2002. Flow of water in rigid and non-rigid, saturated and unsaturated soils. In: Capriz, G. et al., Birkhäuser, Boston, pp. 181–211.

Römkens, M.J.M., Prasad, S.N., 1992. A spectral series approach to infiltration for crusted and not crusted soils. In: Summer, Stewart, (Eds.), Chemical and Physical Processes. Advances in Soil Science. Lewis Publishers, pp. 151–170.

Römkens, M.J.M., Wang, J.Y., Darden, R.W., 1988. A laser microreliefmeter. Trans. ASAE 31, 408–413.

Smiles, D.E., 1974. Infiltration into swelling material. Soil Sci. 117 (3), 140–147.

Smiles, D.E., Rosenthal, M.J., 1968. The movement of water in swelling materials. Aust. J. Soil Res. 6, 237–248.

Wells, R.R. 1995. Effect of cracks on rain infiltration in a Mississippi Delta clay soil. M.S. Thesis. Department of Civil Engineering, University of Mississippi, University, MS.

Wells, R.R. 2003. Wetting and geometry factors affecting shrink/swell soil: Sharkey clay. Ph.D. Dissertation. Department of Biol. and Env. Eng., Cornell University, Ithaca, NY.